Dyes and Pigments 89 (2011) 149–154

Contents lists available at ScienceDirect

Dyes and Pigments

journal homepage: www.elsevier.com/locate/dyepig

Preparation and characterization of bi- and trimetallic titanium based oxides

Mukesh K. Yadav, Ajay V. Kothari, Virendra K. Gupta*

Catalyst & Materials Reliance Technology Centre, Reliance Industries Limited, Hazira, Surat 394 510, India

ARTICLE INFO

Article history:
Received 13 October 2009
Received in revised form
8 October 2010
Accepted 12 October 2010
Available online 21 October 2010

Keywords:
Pigment
Glycolates
TiO_2
$CoTiO_3$
Rutile

ABSTRACT

Rod shaped titanium based glycolates are synthesized by reaction of titanium butoxide with metal acetate (M = Co, Sb, Mn, Ni, Cr) and excess mono ethylene glycol. The products are characterized for composition, morphology and crystalline characteristics. Thermal treatment of metal glycolates led to the preparation of inorganic oxides. Replicated morphology of glycolates is observed for inorganic oxide. Mixed metal oxides are highly crystalline in nature and showed good color characteristics.

1. Introduction

Metal oxides are important class of compounds among the inorganic pigments for different end use applications [1–7]. Titanium dioxide is one of the most widely used pigments due to better light scattering properties, chemical stability and biological inertness. Anatase, rutile and brookite phases of titanium dioxide are synthesized by hydrolysis of titanium precursor such as titanium halides, titanium sulfate, titanium alkoxide using sol-gel, hydrothermal and emulsion methods [8–19]. Further chemical modification of TiO_2 is achieved by incorporation of other metal ion such as Co, Sb, Cr, Mn, Ni [20–22]. Green color cobalt titanate [23,24] is synthesized by solid phase route at elevated temperature [25,26]. Morphological improvement in form of spherical shape is achieved through inorganic precursor methodology [27]. The research is more focused on shape and size control of monometallic materials such as titanium oxide, cobalt oxide and magnesium oxide [28–31]. In present paper, we describe the synthesis and characterization of bimetallic (Ti–Co, Ti–Sb) and trimetallic (Ti–Sb–Mn, Ti–Sb–Cr, Ti–Sb–Ni) glycolates and its oxides.

2. Experimental

2.1. Materials

Titanium n-butoxide (Sigma–Aldrich), cobalt acetate (Labort), antimony acetate (Labort), manganese acetate (Labort), chromium acetate (Labort), ethylene glycol (EG, Reliance Industries Ltd.) and polyvinyl alcohol (PVA, molecular weight 9000–10000, Sigma–Aldrich) were used as received.

2.2. Synthesis

Titanium n-butoxide and metal acetate(s) in stoichiometric amount (Table 1) were mixed with 500 ml of EG. The reaction mixture was stirred for 3 h at 170 °C. The solid product was isolated by centrifuge. It was washed with methanol and dried at 80 °C for 6 h. The synthesized solid product was then heated at 800 °C for 6 h to convert into respective oxide.

Solution stability of the aqueous mixture of bimetallic glycolates is checked under different pH conditions (i.e. 5, 7 and 9). Mixture was stirred for 2 h and the filtrate is checked for metal composition (Table 2). The analysis indicated <5 ppm titanium and <1 ppm cobalt or antimony.

2.3. Characterization

FT–IR spectrum of solid was recorded as KBr pellet using a Perkin–Elmer GX Fourier transform infrared spectrometer with

* Corresponding author. Tel.: +91 261 4135381; fax: +91 261 4135879.
E-mail address: virendrakumar_gupta@ril.com (V.K. Gupta).

0143-7208/$ – see front matter © 2010 Elsevier Ltd. All rights reserved.
doi:10.1016/j.dyepig.2010.10.004

Table 1
Synthesis of bimetallic glycolates.

$Ti(OC_4H_9)_4$ m mol	Metal acetate m mol	Ti:Co or Sb in product[c]
20.5	0[a]	–
15.4	5.1[a]	3.6:1
10.3	10.3[a]	1:1
6.8	13.7[a]	1:1.9
0	20.5[a]	–
10.3	10.3[b]	100:0.2

[a] cobalt acetate.
[b] Sb acetate.
[c] atomic ration by EDX.

Table 2
Elemental composition (ppm) of filtrate of bi- and trimetallic glycolates.

Elements	Ti		Co		Ni		Cr		Mn	
pH treatment	5 pH	9 pH	5 pH	9 pH	5 pH	9 pH	5 pH	9 pH	5 pH	9 pH
Ti:Co = 1:1	2	<1	<1	<1	–	–	–	–	–	–
Ti:Co = 3.6:1	5	<1	2	<1	–	–	–	–	–	–
Ti:Co = 1: 1.9	2	<1	3	<1	–	–	–	–	–	–
Ti:Sb:Ni = 650:1:1	5	<1	–	–	<1	<1	–	–	–	–
Ti:Sb:Cr = 700:2:1	3	<1	–	–	–	–	<1	<1	–	–
Ti:Sb:Mn = 80:10:1	1	<1	–	–	–	–	–	–	1	<1

a resolution of 2 cm^{-1} in the range of 4000 to 400 cm^{-1}. Wide-angle X-ray diffraction (XRD) of samples were carried out using a Bruker D8-Advance diffractometer in the reflection mode at 40 kV and 40 mA with a Cu Kα ($\lambda = 1.5405$ Å) as a radiation source in 2θ range from 2 to 90. SEM images of samples were obtained with FEI Inspect S scanning electron microscope operated at an accelerated voltage of 10–20 kV with working distance of 10 mm. Surface elemental composition of samples were obtained using Oxford INCA EDX analyzer attached with scanning electron microscope at 20 kV. Diffuse reflectance spectra of samples were recorded over Perkin Elmer (Lambda 35) UV–Vis spectrophotometer in the range of 200–1100 nm. Thermal gravimetric analysis (TGA) of samples was conducted in the range of 50–750 °C using Perkin Elmer thermal analyzer under air atmosphere. Color measurement studies were conducted by Hunter lab colorimeter using D25M optical sensor.

2.4. Pigment coating

The synthesized pigment was mixed with 10% aqueous solution of PVA. The mixture was disperse on polymer surface after ultrasonication for 15 min. Coated polymeric surface was dried at 50 °C for 2 h and analyzed for color characteristics.

3. Results and discussion

Bimetallic glycolates (Ti–M; M = Co, Sb) were synthesized by reaction of titanium n-butoxide with metal acetate and ethylene glycol (Scheme. 1). The isolated complexes were found to be stable in acidic as well as alkaline solution (pH from 5 to 9).

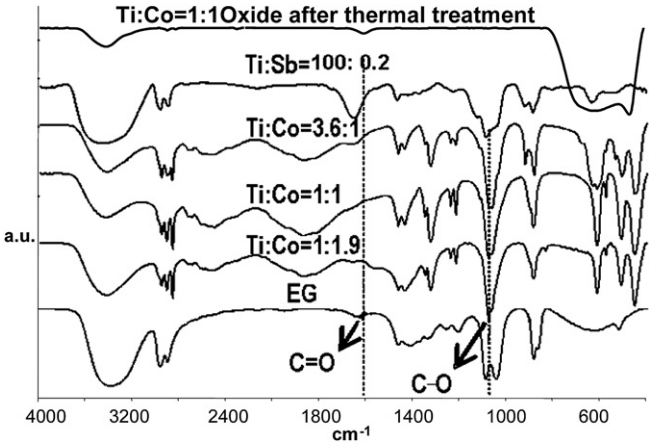

Fig. 1. IR spectrum of bimetallic glycolates of various ratios.

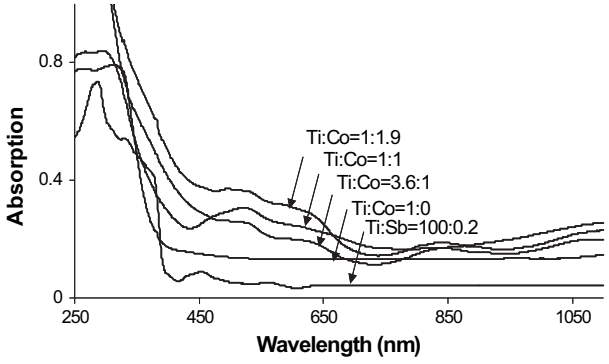

Fig. 2. UV–Vis of bimetallic glycolates of different composition.

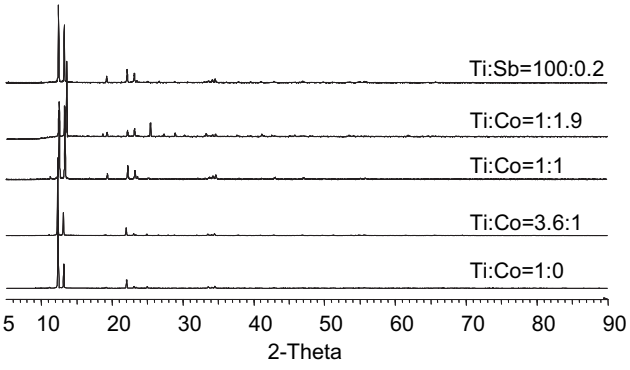

Fig. 3. XRD of bimetallic glycolates of different composition.

The prepared bimetallic glycolates were characterized for spectroscopic (UV, FT–IR), thermal (TGA) and morphological (SEM) characteristics. The FT–IR spectra (Fig. 1) showed absence of C = O absorption at 1750–1650 cm^{-1} assignable to acetate moiety and

$$Ti(OBu)_4 + M(OOCCH_3)_x \xrightarrow[\Delta]{EG} \text{Ti-M glycolate} \xrightarrow{\Delta} \text{Ti-M oxide}$$

M=Co, Sb; x = 2 for Co and 3 for Sb

Scheme. 1. Synthesis of bimetallic glycolates and oxides.

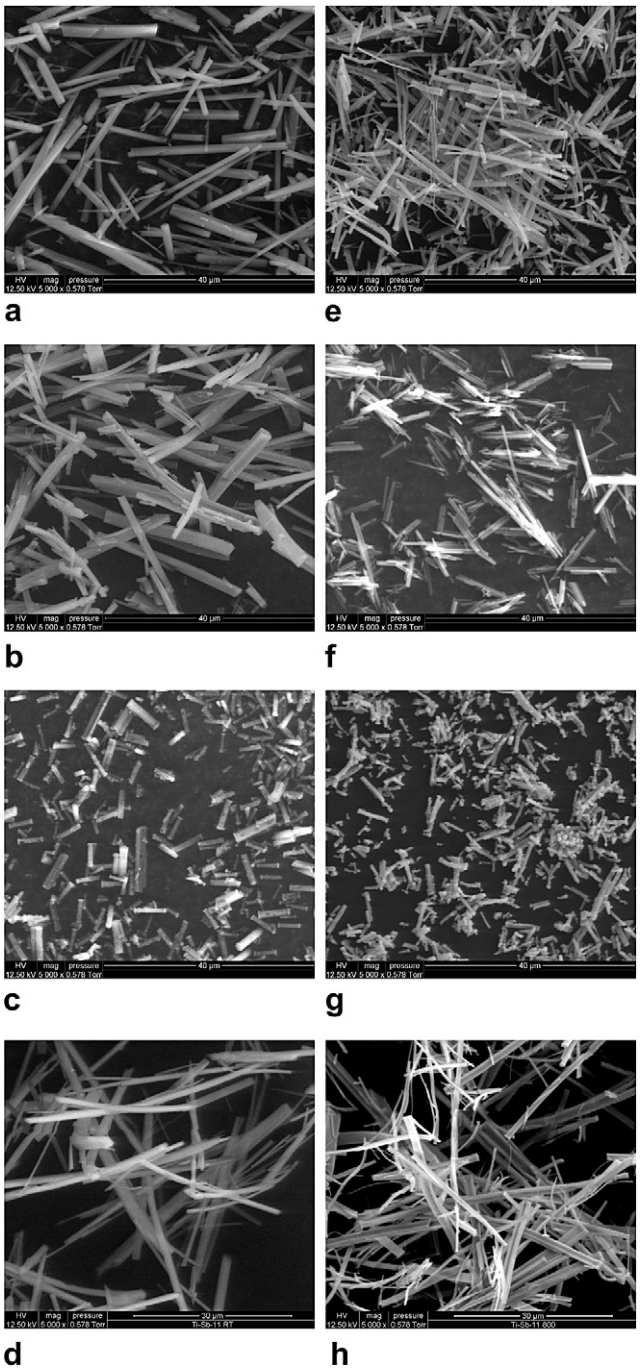

Fig. 4. Morphology of bimetallic glycolates and their oxides (a) Ti:Co-3.6:1 glycolate, (b) Ti:Co-1:1 glycolate, (c) Ti:Co-1:1.9 glycolate, (d) Ti:Sb-1:0.1 glycolate, (e) Ti:Co-3.6:1 oxide, (f) Ti:Co-1:1oxide, (g) Ti:Co-1:1.9 oxide, (h) Ti:Sb-1:0.2 oxide.

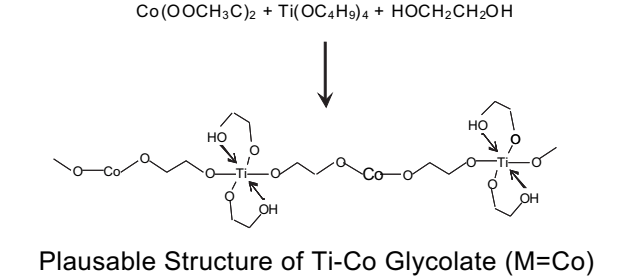

Scheme. 2. Growth of Ti–Co particles.

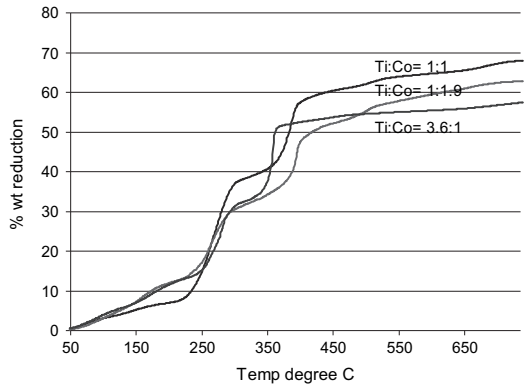

Fig. 5. TGA of Ti–Co bimetallic glycolates of different composition.

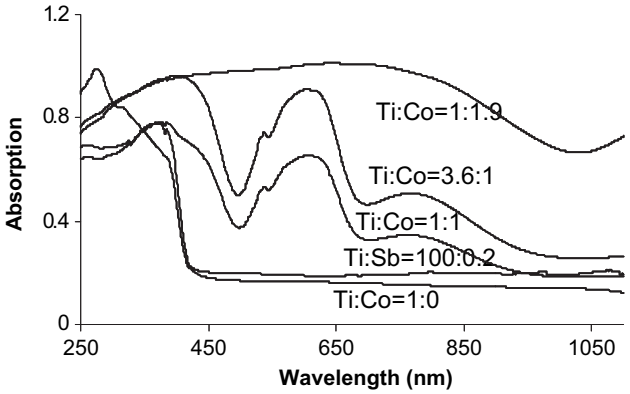

Fig. 6. UV–Vis of bimetallic oxides of different composition.

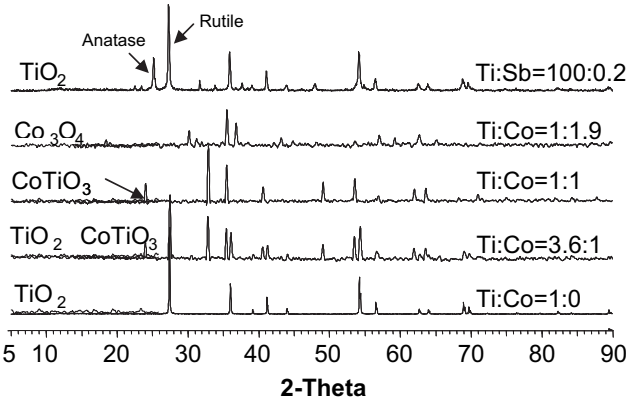

Fig. 7. XRD pattern of bimetallic oxides.

Table 3
Color studies of bimetallic and trimetallic oxides.

Atomic ratio of cation	Color	L	a	b
TiO_2	White	89.37	−0.69	4.05
Ti:Co = 3.6:1	Green	47.05	−16.96	2.03
Ti:Co = 1:1	Green	49.74	−17.5	3.21
Ti:Co = 1: 1.9	Black	19.16	−0.60	0.60
Ti:Sb:Ni = 650:1:1	Yellow	90.42	−3.32	9.08
Ti:Sb:Mn = 80:10:1	Brown	35.21	0.22	10.24
Ti:Sb:Cr = 700:2:1	Buff	76.38	−1.45	27.05

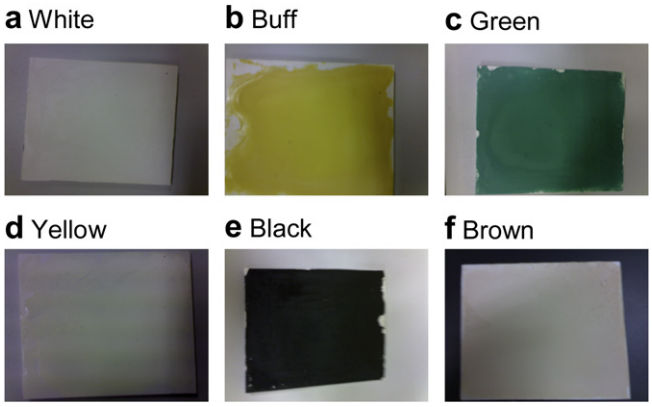

Fig. 8. Coating of pigments over polymeric surface using PVA binder.

presence of vibration band at 1073–1065 cm^{-1} due to C–O–M bond due to formation of metal glycolates. The UV–Vis spectra (Fig. 2) of Ti–Co glycolates showed strong absorptions at 250–350 nm and 430–690 nm due to $O^{2-} \rightarrow Ti^{4+}$ charge transfer transition and tetrahedron Co^{2+} species, respectively. The Ti–Sb complex showed absorption only at 310 nm assignable to $O^{2-} \rightarrow Ti^{4+}$ charge transfer transition. XRD pattern showed (Fig. 3) diffraction lines assigned to Ti–M glycolates species [32]. TGA results of Ti–Co glycolates (Fig. 5) indicated ~10% weight loss up to 220 °C attributable to physical adsorbed EG. The weight loss of 30–35% and 35–50% were observed in the temperature range of 240–300 and 300–450 °C, respectively. The reduction in weight can be attributed to the decomposition of glycolate moiety to yield metal oxides. The morphology of the Ti–Co glycolate complexes showed rod shaped characteristics with diameter from 50 nm to 2 μm (Fig. 4). It is proposed that polymeric bimetallic glycolate is produced (Scheme 2, for Ti–Co glycolate) in rod shaped morphology due to higher growth rate in one direction. Cobalt glycolates are reported to exhibit spherical shape [30] due to uniform growth rates in all the directions. The chain like growth rate is reported for titanium glycolates with rod shape morphology [29].

Mixed oxides were produced by thermal treatment of bimetallic Ti–Co glycolates at high temperature. SEM Studies indicated the replication of rod morphology from glycolate to oxides. IR spectra of calcinied products showed no peaks in the range of 3000–900 cm^{-1} (Fig. 1) indicating decomposition of organic moiety to form inorganic oxides. The UV–Vis spectrum (Fig. 6) showed absorption in the range of 300–500 nm assigned to octahedral $Co^{2+} \rightarrow Ti^{4+}$ inter-valance charge transfer in $CoTiO_3$ [33,34]. Another band in the region of 500–700 nm with λ_{max} at 385 and 602 nm due to 4A2 (F) → 4T1 (F) and 4A2 (F) → 4T1 (P) transitions indicated the presence of tetrahedral Co^{2+} species [34,35]. XRD patterns showed highly crystalline nature of Ti–Co Oxides (Fig. 7). All diffraction lines are well defined and comparable to ICDD database for phase identification. The diffraction pattern of calcined solid with Ti–Co ratio of 3.6:1 showed heterogeneous phases consisting of rutile TiO_2 and $CoTiO_3$. The change of Ti–Co ratio to 1:1 is resulted in the formation of $CoTiO_3$ phase only. $CoTiO_3$ lattice is rhombohedral with R-3 symmetry group having $a = b = 5.06831$ Å, $c = 13.92200$ Å. This is in accordance with PDF pattern no 00-015-0866 and single crystal data [36]. Further change

Table 4
Synthesis of trimetallic glycolates.

Ti $(OC_4H_9)_4$ m mol	Sb $(ac)_2$ m mol	Mn $(ac)_2$ m mol	Ni $(ac)_3$ m mol	Cr $(ac)_3$ m mol	Ti:Sb:X in product[a]
18.1	1.8	1.7	–	–	80:10:1
18.7	1.8	–	1	–	650:1:1
19.1	0.7	–	–	1.3	700:2:1

[a] atomic ration by EDX.

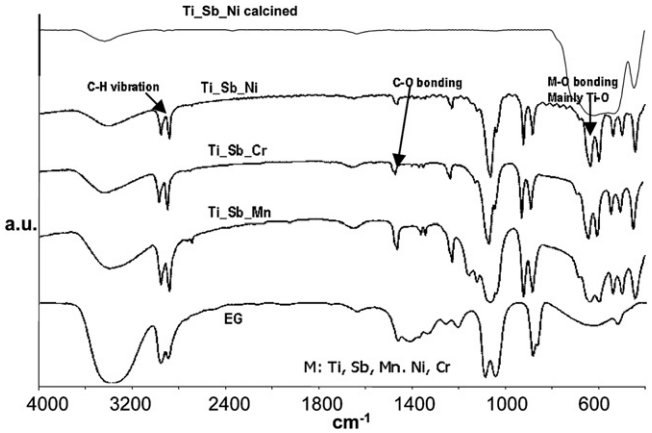

Fig. 9. FT–IR of trimetallic glycolates.

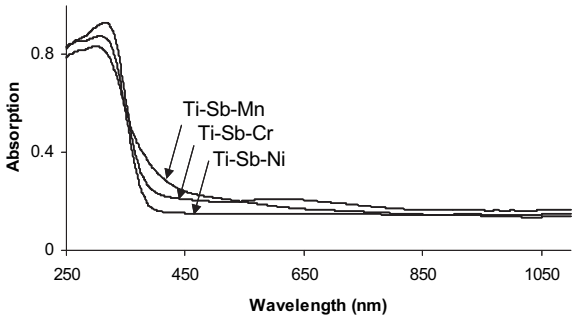

Fig. 10. UV–Vis spectra of trimetallic pigments.

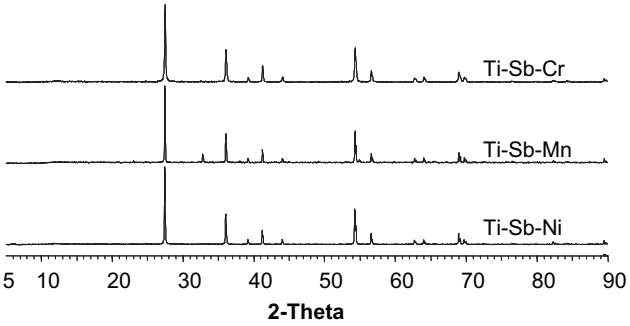

Fig. 11. XRD pattern of trimetallic oxides.

$$Ti(OBu)_4 + Sb(OOCCH_3)_3 + M(OOCCH_3)_x \xrightarrow[\Delta]{EG} \text{Ti-Sb-M glycolate} \xrightarrow{\Delta} \text{Ti-Sb-Moxide}$$

M=Mn, Ni, Cr; x = 2 for Ni, Mn and 3 for Cr

Scheme. 3. Synthesis of trimetallic glycolates and oxides.

Table 5
Color studies of bi- and trimetallic oxides treated with sunlight.

Pigment	L			a			b		
Time (hrs)	6	12	48	6	12	48	6	12	48
TiO_2	90.01	89.92	90.31	0.21	0.52	0.82	3.95	4.25	4.72
Ti:Co = 3.6:1	47.83	48.21	48.68	−16.48	−16.25	−16.68	2.12	2.08	2.41
Ti:Co = 1:1	48.06	48.23	48.46	−18.01	−18.62	−19.15	0.92	0.29	−0.21
Ti:Co = 1: 1.9	19.76	20.18	20.46	−0.46	−0.58	−0.22	0.68	0.54	0.95
Ti:Sb:Ni = 650:1:1	90.89	91.02	91.28	−1.28	−1.83	−1.56	9.51	9.84	9.71
Ti:Sb:Mn = 80:10:1	36.52	37.01	37.77	0.88	0.65	1.02	10.12	10.59	10.97
Ti:Sb:Cr = 700:2:1	76.81	77.41	78.21	−1.01	−1.32	−1.22	27.55	27.09	27.85

in Ti:Co ratio to 1:2 in the precursor showed the formation of Co_3O_4 phase. The presence of $CoTiO_3$ phase is reported to be important for various applications such as pigments [23,24], catalytic materials [33,37,38], high-k gate dielectrics materials [39–42] and sensors for humidity and gas detection [43–46].

Ti:Co oxides are found to exhibit greenish and blackish color characteristics depending on stoichiometric ratio of titanium and cobalt. The color parameter i.e. L, a, b value, of the pigments are shown in Table 3. The Ti–Co oxide with PVA (Polyvinyl alcohol) solution is resulted in the uniform dispersion of pigment over the polymeric surface (Fig. 8). The color characteristics of coated material showed comparable data with respect to pigments.

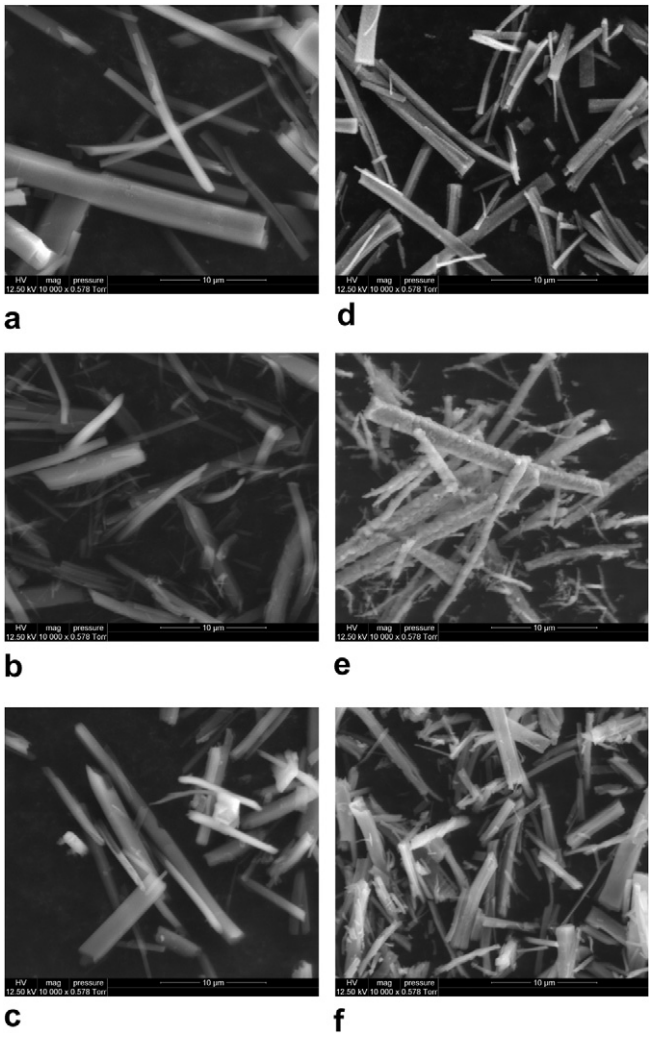

Fig. 12. Morphology of trimetallic glycolates and their oxides (a) Ti–Sb–Ni glycolate, (b) Ti–Sb–Cr glycolate, (c) Ti–Sb–Mn glycolate, (d) Ti–Sb–Ni oxide, (e) Ti–Sb–Cr oxide, (f) Ti–Sb–Mn oxide.

The calcinations of prepared Ti–Sb glycolates are resulted in synthesis of titanium oxide as indicated by XRD pattern. This has led us to synthesize trimetallic complexes (Ti–Sb–Cr, Ti–Sb–Ni, and Ti–Sb–Mn) shown in Scheme 3. The trimetallic glycolates were found to be stable under studied pH conditions (Table 2). EDX analysis of trimetallic products showed the presence of Sb, Cr, Ni and Mn (Table 4). FT–IR (Fig. 9), UV–Vis (Fig. 10) and XRD patterns (Fig. 11) confirmed the formation of trimetallic glycolates. Rod shape morphology is observed for trimetallic glycolates (Fig. 12).

The calcinations of trimetallic glycolates at 800 °C produced mixed oxides. The absence of absorption in the IR spectrum indicates the formation of oxides. The shifting of absorption peak in UV–Vis spectrum towards lower wavelength compared to pure TiO_2 indicates the incorporation of metal ion (Fig. 10). XRD pattern showed crystalline nature of the product (Fig. 11). SEM images (Fig. 12) of the metal oxide indicate the replication of rod-like morphology. Trimetallic oxide showed yellow, buff or brown color depending on metal composition (Table 3).

The trimetallic oxides were dip-coated over polymeric surface using PVA as binder. Color of the pigment is retained after dip coating (Fig. 8). The exposure of coated slide to sunlight indicated the stability of color pigments (Table 5). The addition of moisture on the color surface is, however, found to weaken the coating strength as compared to non-polar solvents such as pentane, hexane due to soluble characteristic of PVA in aqueous medium.

4. Conclusion

Titanium based bimetallic and trimetallic glycolates (Ti–Co, Ti–Sb–Cr, Ti–Sb–Ni, and Ti–Sb–Mn) of rod shape are found to be suitable precursor for corresponding oxide by thermal treatment. Morphology replication phenomenon is observed in mixed metallic oxide from metal glycolates to mixed metallic oxide. The color properties of the mixed oxides are found to be dependant on the composition of the product. Furthermore, inorganic oxides are found to be good pigment for coating over polymeric surface.

References

[1] Buxbaum G, Pfaff G. Industrial inorganic pigments. 3rd ed. Wiley-VCH, Verlag; 2004. p.11.
[2] Sreeram KJ, Kumeresan S, Radhika S, Sundar VJ, Muralidharan C, Nair BU, et al. Use of mixed rare earth oxides as environmentally benign pigments. Dyes and Pigments 2008;76:243–8.
[3] Cavalcante PMT, Dondi M, Guarini G, Raimondo M, Baldi G. Colour performance of ceramic nano-pigments. Dyes and Pigments 2009;80:226–32.
[4] Janes R, Knightley LJ. Synthetic routes to microfine biphasic titania–alumina powders. Dyes and Pigments 2003;56:111–24.
[5] Dondi M, Cruciani G, Balboni E, Guarini G, Zanelli C. Titania slag as a ceramic pigment. Dyes and Pigments 2008;77:608–13.
[6] Cavalcante PMT, Dondi M, Guarini G, Barros FM, Luz AD. Ceramic application of mica titania pearlescent pigments. Dyes and Pigments 2007;74:1–8.

[7] Rao PP, Reddy MLP. $(TiO_2)_1$ $(CeO_2)_{1-x}$ $(RE_2O_3)_x$—novel environmental secure pigments. Dyes and Pigments 2007;73:292–7.
[8] Cassaignon S, Koelsch M, Jolivet JP. From $TiCl_3$ to TiO_2 nanoparticles (anatase, brookite and rutile): thermo hydrolysis and oxidation in aqueous medium. Journal of Physics and Chemistry of Solids 2007;68:695–700.
[9] Yasir VA, MohanDas PN, Yusuff KKM. Preparation of high surface area TiO_2 (anatase) by thermal hydrolysis of titanyl sulphate solution. International Journal of Inorganic Materials 2001;3:593–6.
[10] Sugimoto T, Zhou X, Muramatsu A. Synthesis of uniform anatase TiO_2 nanoparticles by gel–sol method: 3. Formation process and size control. Journal of Colloid and Interface Science 2003;1:43–52.
[11] Bala H, Zhao J, Jiang Y, Ding X, Tian Y, Yu K, et al. A novel approach to synthesis of high-dispersed anatase titania nanocrystals. Materials Letters 2005;59:1937–40.
[12] Baldassari S, Komarneni S, Mariani E, Villa C. Microwave-hydrothermal process for the synthesis of rutile. Materials Research Bulletin 2005;40:2014–20.
[13] Jiang B, Yin H, Jiang T, Jiang Y, Feng H, Chen K, et al. Hydrothermal synthesis of rutile TiO_2 nanoparticles using hydroxyl and carboxyl group-containing organics as modifiers. Materials Chemistry and Physics 2006;98:231–5.
[14] Kim SJ, Lee K, Kim JH, Lee NH, Kim SJ. Preparation of brookite phase TiO_2 colloidal sol for thin film coating. Materials Letters 2006;60:364–7.
[15] Lee BI, Wang X, Bhave R, Hu M. Synthesis of brookite TiO_2 nanoparticles by ambient condition sol process. Materials Letters 2006;60:1179–83.
[16] Srivatsa KMK, Bera M, Basu A. Pure brookite titania crystals with large surface area deposited by Plasma Enhanced Chemical Vapour Deposition technique. Thin Solid Films 2008;516:7443–6.
[17] Paola AD, Cufalo G, Addamo M, Bellardita M, Campostrini R, Ischia M, et al. Photocatalytic activity of nanocrystalline TiO_2 (brookite, rutile and brookite-based) powders prepared by thermohydrolysis of $TiCl_4$ in aqueous chloride solutions. Colloids and Surfaces A: Physicochemical and Engineering Aspects 2008;317:366–76.
[18] Li JG, Ishigaki T, Sun Anatase, Brookite X, Nanocrystals Rutile. Via redox reactions under mild hydrothermal conditions: phase-selective synthesis and physicochemical properties. Journal of Physical Chemistry C 2007;111:4969–76.
[19] Dambournet D, Belharouak I, Amine K. Tailored preparation methods of TiO_2 anatase, rutile, brookite: mechanism of formation and electrochemical properties. Chemistry of Materials 2010;22:1173–9.
[20] Charvat RA. Coloring of plastics fundamentals. 2nd ed. Wiley; 2005. 130.
[21] Lyubenova TS, Ocana M, Carda J. Brown ceramic pigments based on chromium (III)-doped titanite obtained by spray pyrolysis. Dyes and Pigments 2008;79:265–9.
[22] Janes R, Knightley LJ, Harding CJ. Structural and spectroscopic studies of iron (III) doped titania powders prepared by sol-gel synthesis and hydrothermal processing. Dyes and Pigments 2004;62:199–212.
[23] Haines AJ. Infrared reflective wall paints. PCT Patent Application; 2005. WO/2005/095528R.
[24] Fischer R, De Ahna D. Inorganic pigments and process for their production. US Patent 1987; 4696700.
[25] Popov SG, Levitskii VA. Thermodynamics of double oxides. II. Study of the CoO–TiO_2 system by the emf method. Journal of Solid State Chemistry 1981;38:1–9.
[26] Balducci L, Sarti D, Gerelli F. Inorganic pigments and process for preparing. US Patent 1978; 4097300.
[27] Nakamura T. Cobalt titanate particles and process for producing the same. US Patent 1992; 5091012.
[28] Figlarz M, Fievet F, Lagier JP. Process for the reduction of metallic compounds by polyols, and metallic powders obtained by this process. US Patent 1985; 4539041.
[29] Pol VG, Langzam Y, Zaban A. Application of Microwave Superheating for the synthesis of TiO_2 Rods. Langmuir 2007;23:11211–6.
[30] Chakroune N, Viau G, Ammar S, Jouini N, Gredin P, Vaulaya MJ, et al. Synthesis, characterization and magnetic properties of disk-shaped particles of a cobalt alkoxide: $CoII(C_2H_4O_2)$. New Journal of Chemistry 2005;29:355–61.
[31] Makhluf S, Dror R, Nitzen Y, Abramovich Y, Gedanken A. Microwave-Assisted synthesis of nanocrystalline MgO and its use as a bacteriocide. Advanced Functional Materials 2005;15:1708–15.
[32] Jiang X, Wang Y, Herricks T, Xia Y. Ethylene glycol-mediated synthesis of metal oxide nanowires. Journal of Materials Chemistry 2004;14:695–703.
[33] Brik Y, Kacimi M, Ziyad M, Bozon-Veduraz F. Titania-supported cobalt and cobalt–phosphorus catalysts: characterization and performances in ethane oxidative dehydrogenation. Journal of Catalysis 2001;202:118–28.
[34] Zhou GW, Lee DK, Kim YH, Kim CW, Kang YS. Preparation and spectroscopic characterization of ilmenite-type $CoTiO_3$ nanoparticles. Bulletin of Korean Chemical Society 2006;27:368–72.
[35] Verberckmoes A, Weckhuysen BM, Schoonheydt RA. Spectroscopy and coordination chemistry of cobalt in molecular sieves. Microporos and Mesoporous Materials 1998;22:165–78.
[36] Kidoh K, Tanaka K, Marumo F, Takei H. Electron density distribution in an ilmenite-type crystal of cobalt(II) titanium(IV) trioxide. Acta Crystallographica Section B Structural Crystallography and Crystal Chemistry 1984;40:92–6.
[37] Tohji K, Udagawa Y, Tanabe S, Ida T, Ueno A. Catalyst preparation procedure probed by EXAFS spectroscopy. 2. Cobalt on titania. Journal of the American Chemical Society 1984;106:5172–8.
[38] Haber J. Catalysis–where science and industry meet. Pure and Applied Chemistry 1994;66:1597–620.
[39] Pan TM, Lei TF, Chao TS. Comparison of ultrathin $CoTiO_3$ and $NiTiO_3$ high-k gate dielectrics. Journal of Applied Physics 2001;89:3447–52.
[40] Pan TM, Lei TF, Chao TS, Chang KL, Hsieh KC. High quality ultrathin $CoTiO_3$ high-k gate dielectrics. Electrochemical and Solid-State Letters 2000;3:433–4.
[41] Pan YM, Lei TF, Chao TS. High-k cobalt-titanium oxide dielectrics formed by oxidation of sputtered Co/Ti or Ti/Co films. Applied Physics Letters 2001;78:1439–44.
[42] Ahn KY, Forbes L. Low-temperature grown high quality ultra-thin CoTiO3 gate dielectrics. US Patent 2005; 6953730.
[43] He HY. Humidity sensitivity of $CoTiO_3$ thin film prepared by sol-gel method. Materials Technology: Advanced Performance Materials 2007;22:95–7.
[44] Siemons M, Simon U. Preparation and gas sensing properties of nanocrystalline La-doped $CoTiO_3$. Sensor & Actuators B 2006;120:110–8.
[45] Siemons M, Simon U. Gas sensing properties of volume-doped $CoTiO_3$ synthesized via polyol method. Sensor & Actuators B 2007;126:595–603.
[46] Chu X, Liu X, Wang G, Meng G. Preparation and gas-sensing properties of nano-$CoTiO_3$. Materials Research Bulletin 1999;34:1789–95.